THE JOURNAL OF BIOLOGICAL CHEMISTRY
Vol. 271, No. 16, Issue of April 19, pp. 9483–9489, 1996
Printed in U.S.A.

Unexpectedly Strong Binding of a Large Metal Ion (Bi^{3+}) to Human Serum Transferrin*

(Received for publication, December 12, 1995, and in revised form, February 8, 1996)

Hongyan Li, Peter J. Sadler‡, and Hongzhe Sun

From the Department of Chemistry, Birkbeck College, University of London, Gordon House and Christopher Ingold Laboratories, 29 Gordon Square, London WC1H 0PP, United Kingdom

Large metal ions (>0.9 Å ionic radius) have previously been found to bind only weakly to human serum transferrin (hTF, 80 kDa), presumably because the interdomain cleft cannot close around the metal and synergistic anion. Surprisingly, therefore, we report that Bi^{3+} (ionic radius 1.03 Å), a metal ion widely used in anti-ulcer drugs, binds strongly to both the N- and C-lobes with log K_1* = 19.42 and log K_2* = 18.58 (10 mM Hepes, 5 mM bicarbonate, 310 K). The uptake of Bi^{3+} by apo-hTF from bismuth citrate complexes is very slow (hours), whereas that from bismuth nitrilotriacetate is rapid (minutes). Evidence from absorption and NMR spectroscopy is presented to show that Bi^{3+} binds to the specific Fe^{3+} binding sites along with carbonate as the synergistic anion. Under the conditions used, preferential binding of $Bi^{3+}$to the C-lobe of hTF is observed. Linear free energy relationships show that there is a strong correlation between the strength of binding of Bi^{3+} and Fe^{3+} to a wide variety of ligands which include transferrin. Therefore we conclude that the strength of metal ion binding to transferrin is determined more by the ligand donor set than by the size of the ion.

Transferrin (80 kDa) is a serum iron transport glycoprotein with a concentration in blood of ~2–4 mg/ml. Its normal function is to carry iron as Fe^{3+} between sites of uptake, utilization, and storage (1–4). It contains two specific Fe^{3+} binding sites per molecule, each approximately octahedral and consisting of two tyrosinates, one histidine, one aspartate, and a bidentate carbonate anion (the synergistic anion) derived from the buffer (5–7). Iron is situated in N-lobe and C-lobe interdomain clefts, which close around the metal and synergistic anion (4). Apo-hTF[1] is known to bind to a wide variety of metal ions. The strength of binding appears to be dependent on the size of the metal ion, being optimum for Fe^{3+} (ionic radius 0.65 Å), weaker for either slightly smaller, *e.g.* Ga^{3+} (0.62 Å), or slightly larger, *e.g.* In^{3+} (0.80 Å), ions and much weaker for very small, *e.g.* Al^{3+} (0.54 Å), or very large, *e.g.* lanthanide (0.86–1.03 Å) ions (Table I). These data appear to indicate that strong binding arises from the matching of the ionic radius to the size of the binding cleft (4). In the case of the larger ions, the interdomain cleft may not close at all.

Since transferrin is only about 30% saturated with iron in normal serum (8), there is substantial binding capacity for other metal ions that enter the blood. Thus transferrin is an important serum transport agent for metal ions of therapeutic, diagnostic or toxic importance including Al^{3+} (9) Ga^{3+}, In^{3+} (10), and Ru^{3+} (11).

There are no previous reports of the binding of Bi^{3+} to transferrin, although such binding might be expected to be weak on account of the large size of Bi^{3+} (ionic radius 1.03 Å, log $K \sim 5$; predicted from Table I). Bismuth compounds have been used in medicine for more than 200 years for a variety of gastrointestinal disorders (12, 13). There is particular interest in bismuth(III) citrate solubilized by ammonium and potassium hydroxide, which forms the basis of the colloidal bismuth subcitrate present, for example, in the drugs Telen® (Byk Gulden) and De-Nol® (Gist Brocade) (14, 15). Recently a new adduct of ranitidine with bismuth citrate (Glaxo Wellcome plc), which combines the antisecretory action of ranitidine with mucosal protectant and bactericidal properties of bismuth(III), has been granted a product license in the UK (16, 17). There is also interest in using compounds containing radioactive bismuth isotopes as targeted radiotherapeutic agents (18). Despite this medicinal interest, the speciation of bismuth in blood plasma, in particular the binding of Bi^{3+} to blood plasma proteins, is poorly understood.

In this paper we report the first detection of the binding of Bi^{3+} to serum transferrin (19). We determine the binding constants via electronic absorption spectroscopy and show, by absorption and NMR spectroscopy, that Bi^{3+} is taken up into the specific iron sites of transferrin and is accompanied by concomitant binding of the synergistic anion carbonate. We also show that there is preferential uptake into the C-lobe site. Linear free energy plots correlating the strength of binding of Bi^{3+} and Fe^{3+} to a wide variety of ligands provide an insight into the reasons why Bi^{3+} binds tightly to transferrin.

EXPERIMENTAL PROCEDURES

Materials—Apo-hTF was purchased from Sigma (catalog no. T0519) and was washed three times with 0.1 M KCl to remove low molecular mass impurities using Centricon 30 ultrafilters (Amicon). [Bi(Hcit)] was provided by Glaxo Wellcome plc. Crystalline [Bi(NTA)] was synthesized according to a literature procedure (20) and had a satisfactory elemental analysis. $NaHCO_3$ (Aldrich), $NaH^{13}CO_3$ (99% enriched ^{13}C, MSD Isotopes), H_3NTA (Aldrich), and Hepes (Aldrich) were used as received.

A 50 mM stock solution of [Bi(Hcit)] was prepared by adding the minimum amount of ammonia solution to a suspension of [Bi(Hcit)] until it became clear. The final pH of this solution was ~7, and it was then diluted to 1.0 mM before use.

$[Bi(NTA)_x]$ solutions were prepared from a stock solution of

* The costs of publication of this article were defrayed in part by the payment of page charges. This article must therefore be hereby marked "*advertisement*" in accordance with 18 U.S.C. Section 1734 solely to indicate this fact. * This work has been supported by Glaxo Wellcome plc., Biotechnology and Biological Sciences Research Council, and Engineering and Physical Sciences Research Council and by a Committee of Vice-Chancellors and Principals overseas research student award (to H. S.).

‡ To whom correspondence should be addressed: Dept. of Chemistry, University of London, Gordon House and Christopher Ingold Laboratories, London WC1H 0PP, United Kingdom. Tel.: 44-171-380-7480; Fax: 44–171-380-7464; E-mail: ubca424@ccs.bbk.ac.uk.

[1] The abbreviations used are: hTF, human serum transferrin; [Bi(Hcit)], Bi(III) citrate; $[Bi(NTA)_x]$, Bi^{3+} with x mol eq NTA present (does not imply all x mol of NTA bound to Bi); k*, bicarbonate-independent binding constant; NTA, nitrilotriacetate; pH*, pH meter reading in D_2O solution; TOCSY, total correlated spectroscopy; TSP, sodium trimethylsilyl-d_4-propionate.

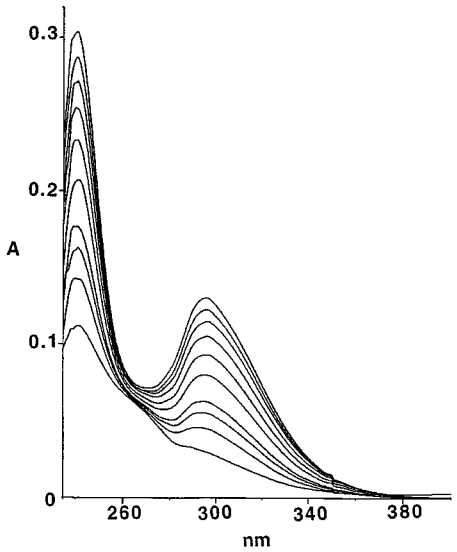

FIG. 1. **Dependence of absorbance (*A*) on time for a solution containing apo-hTF and 2 mol eq [Bi(Hcit)] in 10 mM Hepes buffer solution (5 mM $NaHCO_3$, pH 7.4) at 310 K.** Two new absorbance bands centered at 241 and 295 nm appear and are indicative of Bi^{3+} binding to the specific binding sites of transferrin. Reaction times from bottom to top: 0, 5, 10, 15, 30, 60, 120, 240, 420, and 660 min.

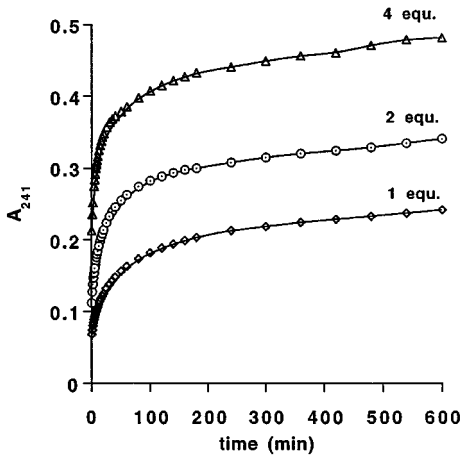

FIG. 2. **Dependence of A_{241} on time for the reaction of apo-hTF with different mol ratios of [Bi(Hcit)] at 310 K.**

[Bi(NTA)] in water (pH ~4.7) by adding the appropriate amount of NTA. The bismuth concentration was determined by inductively coupled-plasma atomic emission spectroscopy (Perkin Elmer).

A solution of $[Fe(NTA)_2]$ was prepared from an iron atomic absorption standard solution (1000 ppm in 1% HNO_3, Aldrich) and 2 mol eq of NTA. The pH was gently raised to 5–6 with microliter amounts of NaOH (1 M). This solution was then further diluted to give the required $[Fe(NTA)_2]$ concentration in 10 mM Hepes buffer.

Preparation of NMR Samples—To allow H-D exchange, apo-hTF was dissolved in 0.1 M KCl in D_2O, and after adjustment of the pH* to 7.25, was left for 4 h at ambient temperature. After lyophilization, the sample was redissolved in D_2O containing 10 mM $NaHCO_3$. The pH* was then readjusted to 7.25 ± 0.05, when necessary, using NaOD and DCl (0.2 M). The pH* values of NMR solutions were recorded before and after NMR measurements.

Samples for UV Spectroscopy—These were prepared by diluting aliquots of a stock apo-hTF solution to ~10^{-5} M with 10 mM Hepes buffer, pH 7.4. The concentration of apo-hTF was determined spectrophotometrically on the basis of ϵ_{280} 93,000 M^{-1} cm^{-1} (21). Immediately before adding Bi^{3+}, an aliquot of a concentrated solution of $NaHCO_3$ (0.25 M) was added to give a 5 mM concentration of HCO_3^-. For kinetic experiments, a solution containing 10 mM Hepes buffer was used for background correction. The spectrum of the apo-hTF solution (containing 5 mM bicarbonate) was recorded after equilibration at 310 K for 10 min. Aliquots of the stock solution of bismuth (usually 5–20 μl of [Bi(Hcit)] or [Bi(NTA)] solutions) were then added to the apo-hTF cuvette, and the spectrum was recorded at various time intervals. For titration experiments (at equilibrium), a similar procedure was used. Each solution was allowed to equilibrate at 310 K for at least 30 min before the spectrum was recorded. The dependence of the stability of bismuth hTF on pH was determined by varying the pH of a solution containing 3 mol eq of [Bi(NTA)] and 10^{-5} M hTF in 5 mM $NaHCO_3$ and recording the UV spectrum after equilibration for 1 h.

NMR Spectroscopy—^1H NMR spectra were recorded on JEOL GSX500 or Varian Unity 600 spectrometers at 500 and 600 MHz, respectively. Spectra were acquired using 0.7 ml of solution in 5 mm tubes at 310 K, using 400-1200 transients, 6-μs (50°) pulses, recycle time 2 s, 16,384 data points, and water suppression via presaturation. The chemical shift reference was TSP via endogenous formate (8.465 ppm, pH* > 7), which was always present in our samples as a minor impurity. Resolution enhancement of the spectra was achieved by processing the FIDs with a combination of unshifted sine-bell and exponential functions (line broadening of 1.5–5 Hz) on a Silicon Graphics computer using Varian VNMR software. A two-dimensional TOCSY spectrum (mixing time 60 ms) of hTF at pH* 7.25 was acquired using 2,048 data points in the f_2 dimension, acquisition time 0.12 s, 48 scans, and 256 increments in the f_1 dimension, in a total time of 14 h.

Proton-coupled ^{13}C NMR spectra were recorded on a JEOL GSX 500 instrument operating at 125 MHz. Typically 10,000–30,000 scans were collected using a pulsewidth of 6 μs (50°), relaxation delay 2 s, 16,384 data points. The spectra were processed using exponential functions (line-broadening of 5–8 Hz). The chemical shift reference was TSP via added internal dioxan (67.4 ppm).

Electronic Absorption Spectroscopy—This was performed on a computer-controlled Perkin-Elmer Lambda 16 spectrometer. The temperature of the cells was maintained at 310 ± 0.1 K using a PTP-1 Peltier temperature programmer.

pH Measurements—These were made using a micro-combination electrode (Aldrich) and a Corning 145 pH meter calibrated with standard buffers at pH 4, 7, and 10.

Calculations—Equilibrium titration curves were initially fitted using the modified Hill plot (22), followed by an iterative procedure similar to that used by Harris and Pecoraro (23) to recalculate K_2. Briefly this involves evaluating the concentrations of free Bi^{3+}, free NTA, and apo-hTF by iteration to minimize differences between calculated and experimentally fixed values of total bismuth, total NTA, and total apo-hTF, assuming a set of values of K_1 (from modified Hill plot) and K_2 for bismuth binding. Values of K_2 were varied to minimize the difference between observed and calculated Δε values. The calculations were carried out using the program Kaleidagraph (Synergy Software).

RESULTS

Electronic Absorption Spectroscopy

The complexation of metal ions to the phenolic groups of the tyrosine residues in the specific metal-binding sites of apo-hTF leads to the production of two new absorption bands at 241 and 295 nm (2). These new bands are readily apparent in difference UV spectra of metal-transferrins and apo-hTF.

Kinetic Studies

Fig. 1 shows time-dependent difference UV spectra of apo-hTF in the presence of 2 mol eq of [Bi(Hcit)] at 310 K in 10 mM Hepes buffer, pH 7.4, 5 mM bicarbonate. The two new absorbance bands that appear at 241 and 295 nm are similar to those reported previously for binding of other trivalent metal ions to apotransferrin (2). The variation in absorbance at 241 nm with time, together with data for reactions involving 1 and 4 mol eq of [Bi(Hcit)], are shown in Fig. 2 .The time dependence of the absorbance at 295 nm is similar. It can be clearly seen that the absorbance increases rapidly within the first 10 min, followed by a slower second phase. With 2 mol eq of [Bi(Hcit)] present, about 50% of total bismuth binding occurs within the first fast phase, and within the next 10 h the remaining 50% binds. With increasing bismuth concentration, the rate of the first phase increases, whereas that of the slower step remains almost the same. Detailed experiments that might allow a full kinetic analysis were not attempted.

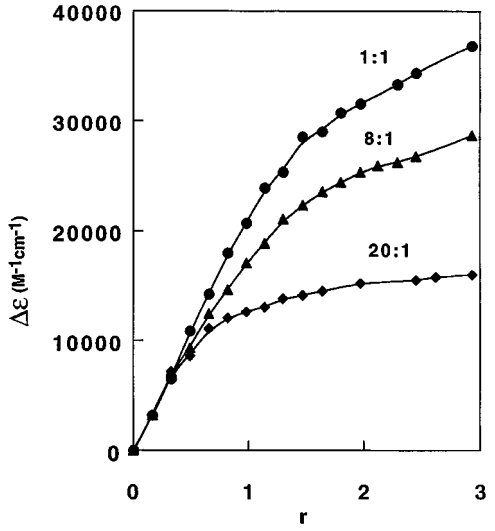

FIG. 3. **Titration curves for addition of [Bi(NTA)$_x$] to 1.09 × 10^{-5} M apo-hTF in 10 mM Hepes buffer at pH 7.4 containing 5 mM bicarbonate, with x = 1, 8, and 20.** $\Delta\epsilon$ equals the absorbance at 241 nm divided by the transferrin concentration; r is the ratio of [Bi] to [hTF].

Under similar conditions, the reaction of apo-hTF with [Bi(NTA)] also gave rise to the same absorbance bands at 241 and 295 nm, but at a much faster rate than that observed for [Bi(Hcit)]. Complete reaction of hTF with 1 or 2 mol eq of [Bi(NTA)] occurred within 30 min (data not shown).

Equilibrium Studies

Apo-hTF was titrated with [Bi(NTA)$_x$] (x = 1, 8, or 20), and the absorbance at 241 nm was monitored. A set of titration curves for NTA:Bi ratios of 1:1 to 20:1 is shown in Fig. 3. For NTA:Bi = 1:1, $\Delta\epsilon$ increases linearly with increase in Bi:hTF ratio (r) until a value of r = ~1 is reached, showing that all the added bismuth is bound to apo-hTF at low values of r. Beyond r = 1, the absorbance increases further but the plot curves downward indicative of the occupation of a second site with a lower binding constant and of competition between free NTA and hTF. With increasing NTA:Bi ratios (8:1 and 20:1), the plots (Fig. 3) show more pronounced downward curvature at high r values due to the competition between hTF and NTA.

The slope of the initial linear portion of these curves is 21,900 (± 650) M^{-1} cm^{-1} and can be equated to the molar absorptivity of transferrin with one site saturated with Bi^{3+} ($\Delta\epsilon_1$). Hence if the two sites are equivalent, a $\Delta\epsilon$ value of ~43,800 M^{-1} cm^{-1} would be expected when both sites are filled. These values are compared to those of other metal-transferrin complexes in Table I.

The absorbance data obtained at different molar ratios of NTA:Bi were used to calculate the binding constants for bismuth-transferrin complexes, using Equations 1 and 2 below.

$$\text{Bi(NTA)} + \text{hTF} = \text{Bi} - \text{hTF} + \text{NTA}$$

$$K_{a1} = \frac{[\text{Bi} - \text{hTF}][\text{NTA}]}{[\text{Bi(NTA)}][\text{hTF}]} \qquad \text{(Eq. 1)}$$

$$\text{Bi(NTA)} + \text{Bi} - \text{hTF} = \text{Bi}_2 - \text{hTf} + \text{NTA}$$

$$K_{a2} = \frac{[\text{Bi}_2 - \text{hTF}][\text{NTA}]}{[\text{Bi(NTA)}][\text{Bi} - \text{hTF}]} \qquad \text{(Eq. 2)}$$

The relationships between the equilibrium constants K_{a1} and K_{a2} and the stability constants for bismuth transferrin (K_1 and K_2) and bismuth NTA are given by the following equations.

$$\text{Bi} + \text{hTF} = \text{Bi} - \text{hTF}$$

TABLE I
Molar absorptivities and metal-transferrin binding constants

Metals	Radius[a]	$\Delta\varepsilon_1$ (λ_{max}/nm)	log K_1*	log K_2*
	Å	M^{-1} cm^{-1}		
Al^{3+}	0.54	14,800 (240)	13.72	12.72
Ga^{3+}	0.62	20,000 (242)	19.75	18.80
Fe^{3+}	0.65	18,000 (240)	21.44	20.34
In^{3+}	0.80	17,200 (245)	18.30	16.44
Sm^{3+}	0.96	21,000 (247)	8.35	6.61
Nd^{3+}	0.98	18,700 (247)	7.31	5.26
Bi^{3+}	1.03	21,900 (241)	19.42	18.58

[a] Radii are taken from Shannon, R. D. (1976) *Acta Crystallogr. Ser. A* **32,** 751–767, and refer to a coordination number of 6.

$$K_1 = \frac{[\text{Bi} - \text{hTF}]}{[\text{Bi}][\text{hTF}]} = K_{[\text{Bi(NTA)}]} \cdot K_{a1} \qquad \text{(Eq. 3)}$$

$$\text{Bi} - \text{hTF} + \text{hTF} = \text{Bi}_2 - \text{hTF}$$

$$K_2 = \frac{[\text{Bi}_2 - \text{hTF}]}{[\text{Bi} - \text{hTF}][\text{hTF}]} = K_{[\text{Bi(NTA)}]} \cdot K_{a2} \qquad \text{(Eq. 4)}$$

If it is assumed that the two binding sites for bismuth on hTF are independent and equivalent, then

$$\frac{1}{Y} = \frac{1}{n} + \frac{1}{nK_a}\frac{[\text{NTA}]}{[\text{Bi(NTA)}]} \qquad \text{(Eq. 5)}$$

where the fractional saturation Y = [Bi-bound]/$[\text{hTF}]_{\text{total}}$, n = average number of bismuth ions bound per transferrin molecule, K_a is the intrinsic binding constant, and $K_{a1} = 2\,K_a$ and $K_{a2} = K_a/2$.

For 20:1 NTA:Bi titration curve, the maximum $\Delta\epsilon$ observed (~18,000) never exceeded the calculated molar absorptivity ($\Delta\epsilon_1$ = 21,900 M^{-1} cm^{-1}) (Fig. 3), even at r = 2.5. This suggested that only one Bi^{3+} ion binds to hTF under these conditions, and so these data were used to calculate K_{a1}. The slope of the plot of $1/Y$ *versus* [NTA]/[Bi(NTA)] gave log K_{a1} = 1.88 ± 0.02 (correlation coefficient r = 0.992, n = 1.01).

From the 8:1 NTA:Bi titration curve, it was possible to use a similar plot to calculate log K_{a1} = 1.87 ± 0.02 (in agreement with that obtained from the 1:20 titration curve) and log K_{a2} = 1.28 ± 0.02 (r = 0.99, n = 1.99).

Using the known value (24) for the stability constant of [Bi(NTA)] of log $K_{\text{Bi(NTA)}}$=17.75 and Equations 3 and 4, pH-independent binding constants of log K_1 = 19.63 and log K_2 = 19.03 were calculated for bismuth hTF. However, there is good evidence that the two binding sites are not in fact equivalent (see below), and therefore the second binding constant was recalculated using the mass balance equation, followed by fitting the apparent absorptivity at each point on the titration curve (the method of Harris and Pecoraro; see "Experimental Procedures"). This was simplified by the initial calculation of K_1 and gave log K_2 = 18.80 ± 0.05, a value 0.2 log units smaller than that obtained from the Hill plot (Equation 5). The fitting procedure is very sensitive to the value of K_2, and hence the difference in binding constants between the two sites does not arise from experimental errors. This confirms that the two Bi^{3+} sites are non-equivalent. The difference in binding constants of log K_1 − log K_2 = 0.84 is similar to that reported for Al^{3+}, Ga^{3+}, and Fe^{3+} (Table I).

The bicarbonate-independent binding constants (K*) were calculated from the relationship (25) shown by Equation 6,

$$\log K^* = \log K + \log \alpha_c \qquad \text{(Eq. 6)}$$

where α_c represents the fractional saturation of the apo-hTF binding sites with bicarbonate.

$$\alpha_c = \{K_c[\text{HCO}_3^-]\}/\{1 + K_c[\text{HCO}_3^-]\} \qquad \text{(Eq. 7)}$$

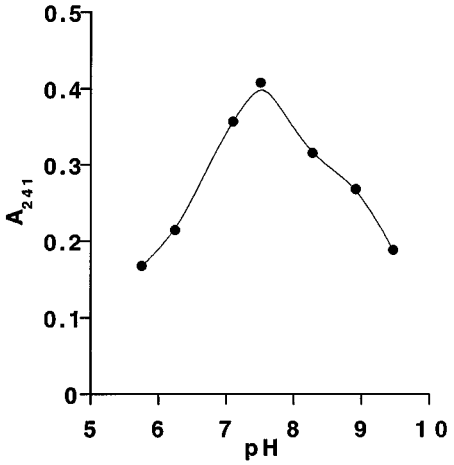

FIG. 4. **Dependence of absorbance on pH for a sample of hTF saturated with Bi^{3+}.**

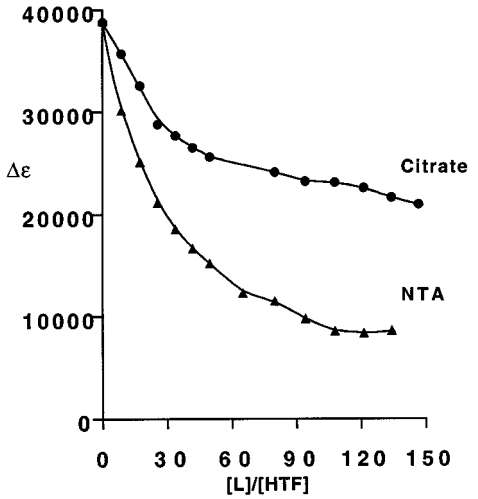

FIG. 5. **Graphs showing the changes in extinction coefficient at 241 nm of bismuth transferrin with increasing citrate or NTA (L) concentrations, at 310 K, pH 7.4.** This experiment was carried out by first adding ~3.0 mol eq Bi(NTA) to apo-hTF to form Bi_2-hTF, followed by titration with free NTA or citrate. Each solution was allowed to equilibrate for 30 min before recording the absorbance.

With 5 mM bicarbonate, pH 7.4, $\alpha_c = 0.6$, giving $\log K^*_1 = 19.42$ and $\log K^*_2 = 18.58$.

Competition Reactions

Effect of pH on Bi^{3+} Binding—The variation of the absorbance at 241 nm with the pH of a solution containing apo-hTF (10 μM), 3 mol eq [Bi(NTA)] (*i.e.* both sites occupied with Bi^{3+}) and 5 mM bicarbonate in 10 mM Hepes buffer, pH 7.4, was investigated. As shown in Fig. 4, the optimum pH for Bi^{3+} binding is ~7.5, and an increase or decrease in pH decreases the absorbance at 241 nm.

Ligand Competition—The competition between hTF and NTA for Bi^{3+} binding was compared to that of citrate. Large excesses of NTA remove Bi^{3+} from both binding sites, whereas even a 140-fold excess of citrate removes only one of the two bound Bi^{3+} ions from transferrin (Fig. 5). NTA would be expected to be more effective in removing Bi^{3+} from transferrin compared to citrate on the basis of the reported stability constants for Bi^{3+} citrate and NTA complexes (log K 13.48 and 17.75 (24), respectively).

Competition with Fe^{3+}—When $[Fe(NTA)_2]$ was added to a solution of apo-hTF containing a 20-fold molar excess of [Bi(NTA)], a new broad band in the visible region centered at ~470 nm gradually increased in intensity (Fig. 6). This band has previously been assigned to a phenolate (π)-metal ($d\pi^*$) transition of Fe^{3+}-hTF (26). Three mol eq of $[Fe(NTA)_2]$ were sufficient to completely displace bismuth from hTF showing that Fe^{3+} binds more tightly to hTF than Bi^{3+}. In accordance with this, when we added excess (up to 20 mol eq) of [Bi(NTA)] to Fe_2-hTF, there was no evidence for iron displacement from the protein.

^{13}C NMR Studies

These were carried out to investigate whether the binding of Bi^{3+} to hTF also involves concomitant binding of carbonate as synergistic anion. Fig. 7 shows the carbonyl region of the ^{13}C NMR spectrum of hTF in the presence of $H^{13}CO_3^-$ (10 mM, enriched to >99% in ^{13}C), and after addition of 0.89 and 2.0 mol eq of Bi^{3+} (as [Bi(NTA)]). In the absence of Bi^{3+}, a sharp signal at 161.1 ppm due to $H^{13}CO_3^-$ is observed, together with a broad envelope at 170–183 ppm corresponding to the backbone and side-chain carbonyls of hTF (natural abundance ^{13}C). When Bi^{3+} is present, a new peak assignable to bound $^{13}CO_3^{2-}$ is observed at 165.8 ppm. The intensity of this peak increases on addition of the second equivalent of Bi^{3+}, suggesting that both sites contain bound carbonate. Addition of the anti-ulcer drug ranitidine bismuth citrate to a similar solution of hTF (allowed to equilibrate overnight) produced the same spectral changes. Although the ^{13}C NMR spectrum showed that most of the free bicarbonate was readily removed from bismuth hTF solutions by ultrafiltration, this procedure had little effect on the peak for bound carbonate (data not shown).

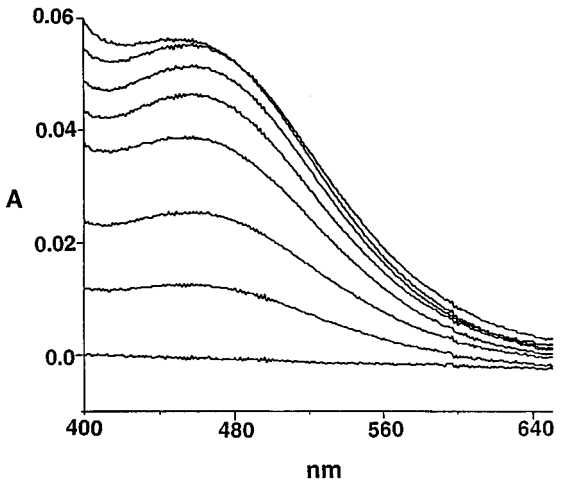

FIG. 6. **Changes in the visible absorption spectrum after addition of various amounts of $[Fe(NTA)_2]$ to a solution of hTF (10 μM) in 10 mM Hepes buffer pH 7.4, containing 5 mM bicarbonate and 20 mol eq [Bi(NTA)] (*i.e.* both metal sites saturated with Bi^{3+}).** From *bottom* to *top*: 0, 0.5, 1.0, 1.5, 2.0, 2.5, 3.0, and 4.0 mol eq $[Fe(NTA)_2]$. Solutions were allowed to equilibrate for 30 min at 310 K after iron addition before the spectrum was recorded.

^{1}H NMR Studies

These experiments were carried out in order to determine the order of lobe loading and to investigate bismuth-induced structural changes in hTF. The 500-MHz ^1H NMR spectrum of hTF in the presence of 10 mM bicarbonate was recorded after addition of 0–2 mol eq of [Bi(NTA)] in steps of 0.5 mol eq. In the high field region, between 0.4 and −1.2 ppm, some peaks, for example *peaks a*, *e*, *g*, and *h*, are unchanged throughout the titration (Fig. 8*A*), whereas others either decrease (*peak c*) or increase (*peak d*) in intensity on addition of the first equivalent of Bi^{3+} and then show no further change on addition of the second equivalent. The most noticeable change in the aromatic

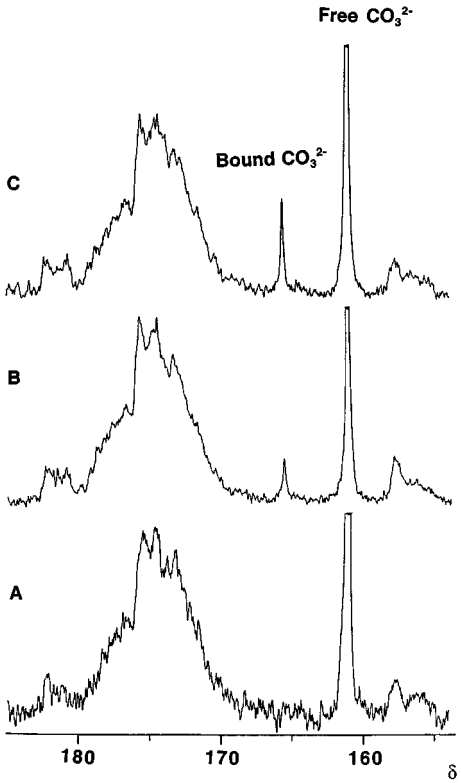

FIG. 7. **125 MHz ^{13}C NMR spectra of hTF (0.9 mM, 50% H_2O, 50% D_2O, pH* 7.25) in the presence of 10 mM $H^{13}CO_3^-$ (*A*), and with addition of 0.89 mol eq [Bi(NTA)] (*B*) and after addition of 2 mol eq [Bi(NTA)] (*C*).**

region of the spectrum is the decrease in intensity of *peak q* (6.34 ppm) and increase in intensity of *peak q′* during addition of the first equivalent of Bi^{3+} (Fig. 8*B*).

A two-dimensional TOCSY ^1H NMR spectrum of apo-hTF in presence of 10 mM bicarbonate, pH* 7.25 showed a cross-peak at 6.34(*peak q*)/7.72 ppm, suggesting that this may arise from a CϵH/CδH connectivity of the imidazole ring of a histidine residue. Furthermore, in the His CϵH region (7.5–8.8 ppm, Fig. 8*B*), peaks *s′*, *t′*, and *j′* appear on addition of the first equivalent of Bi^{3+} but remain almost unchanged with the second equivalent, whereas *peak y* decreases in intensity gradually throughout the titration.

The most intense peaks in the region of the spectrum from ~2.0 to 2.2 ppm are likely to arise from the *N*-acetyl groups of the glycan chains in the C-lobe of hTF. On addition of the first equivalent of Bi^{3+} to apo-hTF, a new apparent singlet peak appears at 2.097 ppm, the peak at 2.080 ppm splits into two, and the shoulder at δ 2.038 ppm decreases in intensity (see Fig. 8*C*). These changes occur progressively from 0 to 1 mol eq of Bi^{3+}, and no further changes occur in this region on addition of the second equivalent of Bi^{3+}.

DISCUSSION

There appear to be no previous reports of the binding of transferrin to bismuth, and it might be expected that Bi^{3+} would bind only weakly since it is a large metal ion (six-coordinate ionic radius 1.03 Å), and ions of this size, such as the lighter lanthanide ions, have previously been found to bind ~10^{12} times more weakly than Fe^{3+} (Table I). The concept has arisen that transferrin cannot exhibit the same closed structure with large metal ions bound because the interdomain clefts cannot close (4). Surprisingly, therefore, our data show that there is strong binding of Bi^{3+} to human serum transferrin.

The changes in the UV spectra of hTF on binding of Bi^{3+} are similar to those observed previously for the binding of other metal ions to the specific Fe^{3+} binding sites. The new bands at 241 and 295 nm are attributable to binding to tyrosine ligands (π-π^* transitions). From the magnitude of the change in extinction coefficient (Table I and Fig. 3), it can deduced that two tyrosines are involved in binding Bi^{3+} in both the N- and C-lobes (Tyr-95/Tyr-188, and Tyr-426/Tyr-517) as is the case for Fe^{3+}. The displacement of Bi^{3+} from transferrin by Fe^{3+}, and lack of binding to Fe_2-hTF provided further evidence for specific binding of Bi^{3+} to the protein. Moreover the ^{13}C NMR data show that carbonate is directly bound to Bi^{3+} in each lobe. Therefore Bi^{3+} can now be added to Cr^{3+}, VO^{2+}, Mn^{3+}, Co^{3+}, Cu^{2+}, Ga^{3+}, and In^{3+} as metal ions that satisfy the criteria (4, 25) for specific metal binding to transferrin.

The two binding constants that we have determined for Bi^{3+} binding to transferrin are only slightly lower than those for Ga^{3+} binding (Table I). Several other previous studies have demonstrated the non-equivalence of the two transferrin binding sites, *e.g.* by NMR (27–32) and EPR (21, 34). The strength of Bi^{3+} binding to transferrin is not so surprising when a linear free energy relationship (LFER) is used to compare the binding constants for Bi^{3+} with those of Fe^{3+} and a wide range of O,N-donor ligands, Fig. 9. There is a good correlation, which is described by Equation 8, with correlation coefficient $r = 0.979$.

$$\log K_{Bi} = -0.906 + 1.172(\log K_{Fe}) \quad \text{(Eq. 8)}$$

The slope of the LFER is greater than 1.0, and many of the stability constants for Bi^{3+} complexes are greater than those of Fe^{3+}. However, the oxygen ligands in the plot are carboxylates and not phenolates, and the former might favor Bi^{3+} since they are softer donors. The two bismuth-hTF binding constants are roughly within the LFER region, although the values are 3 log units lower than predicted, *i.e.* hTF should bind Bi^{3+} more strongly than Fe^{3+}. However, the slope of the LFER might be lower if more appropriate model complexes containing phenolates could be incorporated. Harris *et al*. have found that hydroxybenzyl-containing ligands provide the best predictors for In-hTF binding constants (25). The recent data of Hancock *et al.* (35) support this argument. They have found that the binding constants of Bi^{3+} and Fe^{3+} with DTPA change from $\log K_{Bi}$ (35.6) > $\log K_{Fe}$ (28.0) to $\log K_{Bi}$ (27.76) < $\log K_{Fe}$ (30.44) when the two terminal carboxylate groups are replaced by phenolate groups. The strength of binding of metal ions to hTF therefore appears to be related more to the type of donor set provided by the protein than to the size of the metal ion.

A critical maximum metal ion radius of 0.8–0.9 Å has been suggested for domain closure to occur (36). Thus it has been suggested that the interdomain cleft is open when Ce^{3+} (r = 1.01 Å) binds to lactoferrin. In the case of Bi^{3+}, it seems clear from the values of $\Delta\epsilon_{241}$ (Table I and Fig. 3) that two Tyr ligands are bound to Bi^{3+} in each lobe, as is the case with Fe^{3+}. Since the Tyr residues are on domain 2 and an interdomain polypeptide strand, such binding could occur without domain closure (37).

It would therefore be interesting to study bismuth hTF by x-ray scattering to determine the radius of gyration for comparison with other metallotransferrins (38, 39).

The NMR studies show that (bi)carbonate binds to both the N- and C-lobes of hTF concomitantly with Bi^{3+}. The ^{13}C shift of the bound synergistic anion (165.8 ppm) is close to that observed previously for other metallotransferrins, *e.g.* 166.0/166.2 ppm for Tl^{3+} (40), 165.4 ppm for Al^{3+}, and 166.5 ppm for Ga^{3+} (41), suggesting a similar mode of binding, probably as a bidentate carbonate ion. The anion is strongly bound to bismuth hTF and is not readily removed by dialysis. Studies of

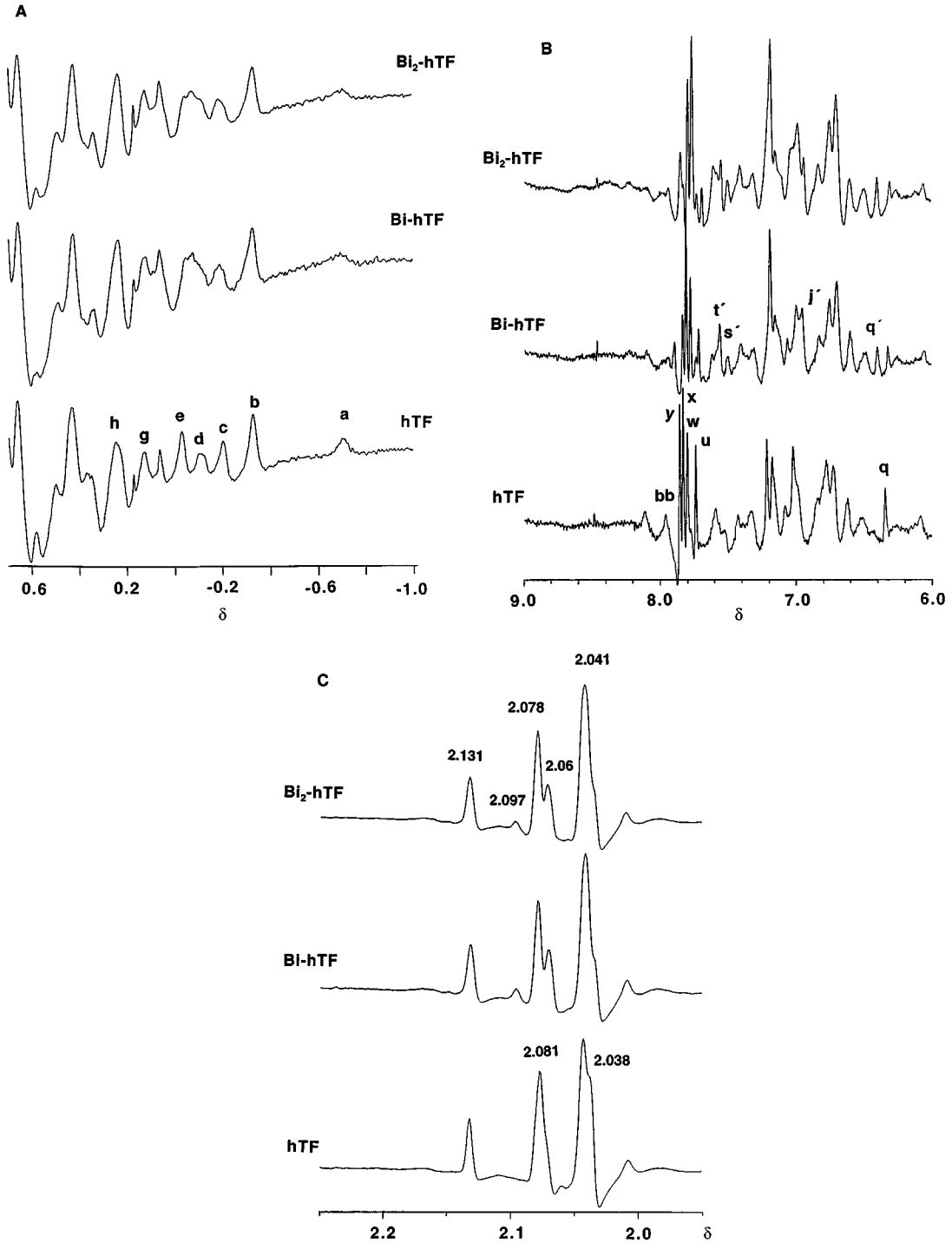

FIG. 8. **Resolution-enhanced 500-MHz ^{1}H NMR spectra of apo-hTF (0.5 mM) in 0.1 M KCl, pH* 7.25 in the high field region (*A*), the aromatic region (*B*), and *N*-acetyl region (*C*), before (*bottom*) and after addition of 1 (*middle*) and 2 (*top*) mol eq of [Bi(NTA)].**

Bi^{3+} binding to transferrin can also be readily monitored by ^{1}H NMR since apo-hTF and Bi-hTF are in slow exchange on the NMR time scale (indicative of strong Bi^{3+} binding). Peaks in both the aromatic and the methyl regions of the spectrum suggest preferential binding of Bi^{3+} to the C-lobe. The relatively sharp *peak q* at 6.34 ppm is affected by the first mol eq of Bi^{3+} and has been previously assigned to a C-lobe residue (42). It has an associated low pK_a (5.87) and an unusual pH titration shift range (0.75 ppm), and arises from a His Cδ proton (based on two-dimensional TOCSY data) with an unusual high field shift. From examination of the x-ray structure of hTF with Fe^{3+} in the C-lobe (7), possible candidates are His-473 or His-535. The sharp resonances at 2.0–2.1 ppm are attributable to the *N*-acetyls of the NAcGlc and NAcNeu residues in each of the two biantennary glycan chains attached to Asn-413 and Asn-611 in the C-lobe of hTF. Since these resonances were perturbed only on addition of the first mol eq of Bi^{3+}, we can conclude that preferential binding occurs to the C-lobe of hTF. A similar NMR behavior has been observed for Ga^{3+} (with oxalate as synergistic anion) and In^{3+} binding to hTF (28, 43), and several other metal ions are known to bind more strongly to the C-lobe of hTF than to the N-lobe (40).

No attempt was made to investigate the kinetics of reactions of hTF with Bi^{3+} citrate or NTA complexes at this stage, but it

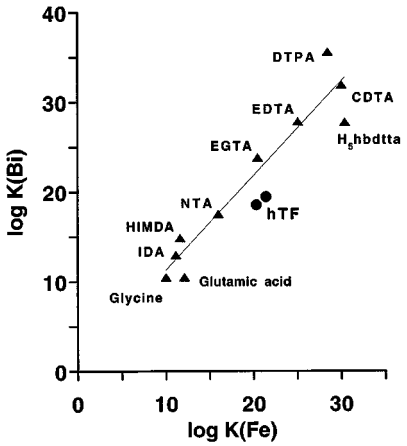

FIG. 9. **Linear free energy relationships (*LFER*) for the complexation of Bi^{3+} and Fe^{3+} with oxygen and nitrogen donors.** These data were taken from Ref. 24. The points for the two binding constants of transferrin are shown as *solid circles*. *CDTA*, *trans*-1,2-diaminocyclohexane; *DTPA*, diethylenetriaminepentaacetic acid; ; *H_5hbdtta*, *N,N′*-bis(2-hydroxybenzyl)diethylenetriamine-*N,N′,N″*-triacetic acid; *HIMDA*, *N*-(2-hydroxyethyl)iminodiethanoic acid; *IDA*, iminodiethanoic acid.

is apparent that there at least two distinct kinetic steps. The citrate complex reacts much more slowly with hTF than the NTA complex, and dissociation of the low molecular mass ligand bound to Bi^{3+} appears to be partly rate-determining. Similar observations have been reported for Fe^{3+} binding to hTF (33, 44).

Conclusions—We expected the binding of Bi^{3+} to transferrin to be weak because the size of the binding cleft is thought to be matched to that of the metal ion, being optimum for Fe^{3+} (ionic radius 0.65 Å). Unexpectedly, therefore, we have found that Bi^{3+} (radius 1.03 Å) binds very tightly to both the N- and C-lobes of transferrin with affinities close to those of the smaller metal ions Ga^{3+} (0.62 Å) and In^{3+} (0.80 Å). Hence, ionic size can now be said not to be the major factor determining the strength of metal binding to transferrin. Linear free energy relationships for the binding of Fe^{3+} and Bi^{3+} to a range of different ligands demonstrate that the ligand donor set plays a dominant role.

We have shown that Bi^{3+} binds specifically to the Fe^{3+} binding sites in transferrin and that (bi)carbonate is also bound as the synergistic anion. Although Bi^{3+} binds relatively strongly, it can be displaced by Fe^{3+}. The NMR data show that Bi^{3+} binds preferentially to the C-lobe, as has been found for several other metal ions. The ligands already bound to Bi^{3+} play an important role in determining the rate of transfer of Bi^{3+} from low molecular mass complexes onto transferrin.

It will be of interest for future work to investigate whether the domains of the N- and C-lobes close around the large Bi^{3+} ions when the metal is bound, and to determine whether Bi^{3+} binding occurs in intact blood plasma or other fluids and whether transferrin plays any role in determining the biodistribution of bismuth in the body.

Acknowledgments—We thank the University of London Intercollegiate Research Service and Medical Research Council Biomedical NMR Centre at Mill Hill, for the provision of NMR facilities, and B. Keohane (Birkbeck College) for assistance with inductively coupled-plasma atomic emission spectroscopy.

REFERENCES

1. Brock, J. H. (1985) in *Metalloproteins: Part 2* (Harrison, P. M., ed) pp. 183–262, Macmillan Press, Basingstoke, United Kingdom
2. Harris, D. C., and Aisen, P. (1989) in *Iron Carriers and Iron Proteins* (Loehr, T. M., ed) pp. 239–351, VCH, Weinheim, Germany
3. Chasteen, N. D. and Woodworth, R. C. in *Iron and Iron Storage* (Ponka, P., Schulman, H. M., and Woodworth, R. C., eds) pp. 69–82, CRC Press, Inc., Boca Raton, FL
4. Baker, E. N. (1994) *Adv. Inorg. Chem.* **41,** 389–463
5. Bailey, S., Evans, R. W., Garratt, R. C., Gorinsky, B., Hasnain, S., Horsburgh, C., Jhoti, H., Lindley, P. F., Mydin, A., Sarra, R., and Watson, J. L. (1988) *Biochemistry* **27,** 5804–5812
6. Sarra, R., Garratt, R., Gorinsky, B., Jhoti, H., and Lindley, P. F. (1990) *Acta Crystallogr. Ser. B* **46,** 763–771
7. Zuccola, H. A. (1993) *The Crystal Structure of Monoferric Human Serum Transferrin.* Ph.D. thesis, Georgia Institute of Technology
8. Leibman, A., and Aisen, P. (1979) *Blood* **53,** 1058–1065
9. Martin, R. B. (1992) in *Aluminum in Biology and Medicine* (Chadwick, D. J., and Whelan, J., eds) pp. 18–25, John Wiley & Sons, New York
10. Welch, M. J. and Moerlein, S. (1980) in *Inorganic Chemistry in Biology and Medicine* (Martell, A. E., ed) pp. 121–140, American Chemical Society, Washington, D. C.
11. Kratz, F., Hartmann, M., Keppler, B. K., and Messori, L. (1994) *J. Biol. Chem.* **269,** 2581–2588
12. Baxter, G. F. (1989) *Pharm. J.* **243,** 805–810
13. Baxter, G. F. (1992) *Chem. Br.* **28,** 445–448
14. Herrmann, W. A., Herdtweck, E., and Pajdla, L. (1991) *Inorg. Chem.* **30,** 2579–2581
15. Asato, E., Katsura, K., Mikuriya, M., Fujii, T., and Reedijk, J. (1995) *Inorg. Chem.* **34,** 2447–2454
16. Clitherow, J. W. (1990) *United Kingdom Patent GB 2220937A*, January 24, 1990
17. Sadler, P. J., and Sun, H. (1995) *J. Chem. Soc. Dalton Trans.* 1395–1401
18. Kozak, R. W., Waldmann, T. A., Atcher, R. W., and Gansow, O. A. (1986) *Trends Biotechnol.* **4,** 259–264
19. Li, H., Sadler, P. J., and Sun, H. (1995) *J. Inorg. Biochem.* **59,** 105
20. Summers, S. P., Abboud, K. A., Farrah, S. R., and Palenik, G. J. (1994) *Inorg. Chem.* **33,** 88–92
21. Chasteen, N. D., White, L. K., and Campbell, R. F. (1977) *Biochemistry* **16,** 363–368
22. Raymond, C. (1981) *Physical Chemistry with Application to Biological Systems*, 2nd Ed., pp. 247–251, Macmillan Publishing Co., Inc. New York
23. Harris, W. R., and Pecoraro, V. L. (1983) *Biochemistry* **22,** 292–299
24. Pettit, G., and Pettit, L. D. (1993) *IUPAC Stability Constants Database*, IUPAC/Academic Software, Otley, United Kingdom
25. Harris, W. R., Chen, Y., and Wein, K. (1994) *Inorg. Chem.* **33,** 4991–4998
26. Patch, M. G., and Carrano, C. J. (1981) *Inorg. Chim. Acta* **56,** L71–L73
27. Kubal, G., Sadler, P. J., and Evans, R. W. (1992) *J. Am. Chem. Soc.* **114,** 1117–1118
28. Kubal, G., Mason, A. B., Patel, S. U., Sadler, P. J., and Woodworth, R. C. (1993) *Biochemistry* **32,** 3387–3395
29. Kubal, G., Mason, A. B., Sadler, P. J., Tucker, A., and Woodworth, R. C. (1992) *Biochem. J.* **285,** 711–714
30. Aramini, J. M., and Vogel, H. J. (1993) *J. Am. Chem. Soc.* **115,** 245–252
31. Aramini, J. M., and Vogel, H. J. (1994) *J. Am. Chem. Soc.* **116,** 1988–1993
32. Aramini, J. M., McIntyre, D. D., and Vogel, H. J. (1994) *J. Am. Chem. Soc.* **116,** 11506–11511
33. El Hage Chahine, J. M., and Fain, D. (1993) *J. Chem. Soc. Dalton Trans.* 3137–3143
34. Harris, A. W., and Sephton, R. G. (1977) *Cancer Res.* **37,** 3634–3638
35. Hancock, R. D., Cukrowski, I., Cukrowski, E., Hosken, G. D., Iccharam, V., Brechbiel, M. W., and Gansow, O. (1994) *J. Chem. Soc. Dalton Trans.* 2679–2685
36. Smith, C. A., Ainscough, E. W., Baker, H. M., Brodie, A. M., and Baker, E. N. (1994) *J. Am. Chem. Soc.* **116,** 7889–7890
37. Lindley, P. F., Bajaj, M., Evans, R. W., Garratt, R. C., Hasnain, S. S., Jhoti, H., Kuser, P., Neu, M., Patel, K., Sarra, R., Strange, R., and Walton, A. (1993) *Acta Crystallogr. Ser. D* **49,** 292–304
38. Grossman, J. G., Neu, M., Pantos, E., Schwab, F. J., Evans, R. W., Townes-Andrews, Lindley, P. F., Appel, H., Thies, W. G., and Hasnain, S. S. (1992) *J. Mol. Biol.* **225,** 811–819
39. Castellano, A. C., Barteri, M., Castagnola, M., Bianconi, A., Borghi, E., and Della Longa, S. (1994) *Biochem. Biophys. Res. Commun.* **198,** 646–652
40. Aramini, J. M., Krygsman, P. H., and Vogel, H. J. (1994) *Biochemistry* **33,** 3304–3311
41. Bertini, I., Luchinat, C., Messori, L., Scozzafava, A., Pellacani, G., and Sola, M. (1986) *Inorg. Chem.* **25,** 1782–1786
42. Kubal, G., Sadler, P. J., and Tucker, A. (1994) *Eur. J. Biochem.* **220,** 781–787
43. Beatty, E. J. (1995) *Recognition of Metal Ions and Anions by the N-lobe of Human Serum Transferrin,* Ph.D. thesis, University of London
44. Bates, G. W., and Wernicke, J. (1971) *J. Biol. Chem.* **246,** 3679–3685